

<sup>24</sup>R. M. Sternheimer, in *Methods of Experimental Physics*, edited by L. C. L. Yuan and C. S. Wu (Academic, New York, 1961), Vol. 5A, pp. 4-55.

<sup>25</sup>E. H. Bellamy, R. Hofstadter, W. L. Lakin, J. Cox, M. L. Perl, W. T. Toner, and T. F. Zipf, *Phys. Rev.* **164**, 417 (1967).

<sup>26</sup>D. W. Aitken, W. L. Lakin, and H. R. Zulliger, *Phys. Rev.* **179**, 393 (1969).

<sup>27</sup>P. J. McNulty and F. J. Congel, *Phys. Rev. D* **1**, 3041 (1970). See also F. J. Congel and P. J. McNulty, *ibid.* **176**, 1615 (1968).

<sup>28</sup>V. N. Tsytoich, *Dokl. Akad. Nauk SSSR* **144**, 310 (1962) [*Sov. Phys. Doklady* **7**, 411 (1962)]; *Zh. Eksperim. i Teor. Fiz.* **42**, 457 (1962); **43**, 1782 (1962) [*Sov. Phys. JETP* **15**, 320 (1962); **16**, 1260 (1962)].

PHYSICAL REVIEW B

VOLUME 3, NUMBER 11

1 JUNE 1971

## Electric-Field-Gradient Calculations in the Aluminum Silicates ( $\text{Al}_2\text{SiO}_5$ )<sup>†</sup>

Michael Raymond\*<sup>‡</sup>

*Department of Physics, The University of Chicago, Chicago, Illinois 60637*

(Received 9 November 1970)

The point-multipole model is used to calculate the electric-field-gradient tensors at the eight nonequivalent aluminum sites of the three  $\text{Al}_2\text{SiO}_5$  polymorphs, kyanite (four sites), andalusite (two sites), and sillimanite (two sites). The contribution from induced dipole and quadrupole moments of the oxygen ions is included. The oxygen-ion polarizabilities and the  $\text{Al}^{3+}$  Sternheimer factor are considered as variable parameters to fit NMR measurements of the 34 independent field-gradient components. The best fit (average disagreement 21%) is obtained with  $\alpha_D = 0.5 \text{ \AA}^3$ ,  $\alpha_Q = 0.1 \text{ \AA}^5$ , and  $\gamma_\infty = -4.9$ . The disagreement is roughly the same at all eight sites. With the theoretical  $\gamma_\infty = -2.4$ , and  $\alpha_D = 1.1 \text{ \AA}^3$ ,  $\alpha_Q = 0.1 \text{ \AA}^5$ , the disagreement is 21% at the six octahedral sites but 82% at the five-coordinated site in andalusite, and 103% at the tetrahedral site in sillimanite. The oxygen-dipole contribution is very large; the quadrupole contribution is generally small but not negligible. Two recent refinements of the kyanite structure enable errors due to inaccuracy in the crystal structure parameters to be estimated. The thermal vibrations of the ions determined by x rays are calculated, and their contribution to the field gradients found to be quite small.

### I. INTRODUCTION

The ionic, or point-ion model, has frequently been used for the computation of electric field gradients in predominantly ionic crystals.<sup>1-10</sup> This model represents the charge distribution of a crystal by point multipoles fixed at the lattice sites. Given the crystal structure and the multipole polarizabilities of the ions, the potential distribution can be calculated by summation over the lattice. Field gradients computed in this manner can be compared with values derived from nuclear-quadrupole tensors  $eQV_{ij}^n/h$  at nuclear sites. Here  $Q$  is the nuclear-quadrupole moment and  $V_{ij}^n$  is the field-gradient tensor at the nucleus.  $V_{ij}^n$  is usually related to the calculated external field gradient  $V_{ij}$  by the Sternheimer antishielding factor<sup>11</sup>  $\gamma_\infty$ , i. e.,  $V_{ij}^n = (1 - \gamma_\infty)V_{ij}$ . There often is considerable disagreement between the calculated and measured electric field gradients. This disagreement is usually ascribed to effects of the finite charge distribution of the negative ion, overlap, charge transfer, covalent bonding, etc. In other words, the disagreement is due to the approximations inherent in the ionic model. But in order to make an estimate of the importance of non-ionic effects, it is first necessary to minimize er-

rors in application of the ionic model. These are due to uncertainties in the atomic coordinates and the multipole polarizabilities of the ions. In comparing the theoretical field gradients with experiment results, uncertainties in the nuclear-quadrupole moment and the Sternheimer antishielding factor must be considered. Thermal vibrations of the ions must also be taken into account.<sup>10</sup>

Theoretical calculations are available for the multipole polarizabilities and  $\gamma_\infty$  for free ions, but their values for ions in a crystal cannot be predicted with any accuracy. The best approach is to study a crystal of low symmetry, so that there are a number of field-gradient components. Then the polarizabilities and  $\gamma_\infty$  can be used as variable parameters to fit the observed nuclear-quadrupole coupling data. It has been shown<sup>2,3,8,10,12-14</sup> that the multipole series must include at least the dipole and quadrupole terms. The effects of induced quadrupoles are more often than not ignored. When they have been considered, it has been for crystals<sup>2,3,8,12-14</sup> with too few field-gradient components to use the variable-parameter approach unambiguously. In only one case<sup>10</sup> ( $\text{AlPO}_4$ ) has there been more than one parameter available for comparison.

The crystals with which this paper deals, kyanite,

sillimanite, and andalusite, have 20, 8, and 6 independent field-gradient components, respectively. The atomic coordinates of kyanite have recently been refined by two independent groups.<sup>15,16</sup> Both groups include data on the thermal movement of the ions. These data afford an excellent opportunity for a test of the ionic model.

## II. CRYSTAL STRUCTURES

The crystal structure of kyanite was determined by Naray-Szabo, Taylor, and Jackson.<sup>17</sup> It is described as a distorted cubic close-packed arrangement of oxygen atoms in which 10% of the tetrahedral interstices contain silicon, and 40% of the octahedral interstices contain aluminum. There are chains of aluminum-oxygen groups parallel to the  $c$  axis, formed by octahedra sharing edges with neighbors on either side. The chains are linked together by the silicon tetrahedra and additional aluminum octahedra.

Refinements of the atomic coordinates were performed by Burnham<sup>15</sup> and by de Rango *et al.*<sup>16</sup> The space group is triclinic ( $P\bar{1}$ ); the unit cell includes four formula units  $\text{Al}_2\text{SiO}_5$ . In the structure there are four nonequivalent octahedrally coordinated aluminum sites, Al(1), Al(2), Al(3), Al(4), all having point symmetry 1. There are 10 nonequivalent oxygen positions, also with point symmetry 1.

The structure of andalusite was determined by Taylor.<sup>18</sup> As in kyanite, there are chains of aluminum-oxygen octahedra parallel to the  $c$  axis. These chains are linked by a framework of silicon tetrahedra and five-coordinated aluminum groups. The atomic coordinates were refined by Burnham and Buerger.<sup>19</sup> The space group is orthorhombic ( $Pnmm$ ); the unit cell includes four formula units  $\text{Al}_2\text{SiO}_5$ . The four equivalent octahedrally coordinated aluminum sites Al(1) are on twofold rotation axes parallel to the  $c$  axis of the crystal. The four equivalent five-coordinated Al(2) sites are situated on reflection planes perpendicular to the  $c$  axis. For both Al(1) and Al(2) sites, the  $c$  axis is a principal axis of the electric-field-gradient tensor. There are four nonequivalent oxygen positions. Three of them are on reflection planes perpendicular to the  $c$  axis; the fourth has the general point symmetry 1.

The sillimanite crystal structure was determined by Taylor.<sup>20</sup> Sillimanite, like kyanite and andalusite, contains chains of aluminum octahedra parallel to the  $c$  axis. They are supported by double chains of aluminum and silicon tetrahedra, also parallel to the  $c$  axis. The atomic coordinates were refined by Burnham.<sup>21</sup> The space group is orthorhombic ( $Pbnm$ ); the unit cell includes four formula units  $\text{Al}_2\text{SiO}_5$ . The four equivalent octahedrally coordinated aluminum sites Al(1) are on symmetry centers (point symmetry  $\bar{1}$ ). The four equivalent tetrahedrally coordinated Al(2) sites are on reflection

planes perpendicular to the  $c$  axis. There are four nonequivalent oxygen positions; three of them are on reflection planes perpendicular to the  $c$  axis, and the fourth has the general point symmetry 1.

Projections of the structures of kyanite, andalusite, and sillimanite may be found in Refs. 15, 19, and 21, respectively.

## III. CALCULATIONS

The computation procedure is essentially the one described by Hafner and Raymond.<sup>12</sup> A rectangular coordinate system was introduced into the triclinic unit cell of kyanite. The  $y$  axis was taken to coincide with the crystal  $b$  axis, and the  $z$  axis in the  $b$ - $c$  plane, very nearly along  $c$  (the angle  $\alpha$  between  $b$  and  $c$  is  $89.97^\circ$ ). In orthorhombic andalusite and sillimanite, the  $x$ ,  $y$ , and  $z$  axes are along  $a$ ,  $b$ , and  $c$ , respectively. The transformation matrices are shown in Table I.

We introduce the following notation for the potential coefficients  $V_r^S$ , the potential component  $r$  at site  $S$ .  $V_0^S$  is the potential,  $V_{1-3}^S$  are the first derivatives of the potential along  $x$ ,  $y$ , and  $z$ , and  $V_{4-9}^S$  are the six second derivatives. Similarly,  $Q_r^S$  is the  $r$ th multipole moment at site  $S$ .  $Q_0^S$  is the charge on site  $S$ ,  $Q_1^S = P_x^S$  (dipole moment),  $Q_4^S = Q_{xx}^S$  (quadrupole moment), etc. Only oxygen multipoles are considered, and moments higher than quadrupole are neglected in this calculation.

The relations between the potential and multipole coefficients can be written in the form

$$V_r^S = \sum_{S'} \sum_{r'} K_r^{S'S'} Q_{r'}^{S'}, \quad (1)$$

where  $K_r^{S'S'}$  represents the potential coefficient  $V_r^S$  generated by a unit  $Q_{r'}^{S'}$  multipole. These  $K$  factors are purely crystallographic parameters determined by the lattice dimensions of the crystal and the coordinates of the sites. The polarizabilities are defined by the relations

$$\begin{aligned} Q_r^S &= -\alpha_D V_r^S \quad (r=1-3) \text{ dipole polarizability,} \\ Q_r^S &= -\alpha_Q V_r^S \quad (r=4-9) \text{ quadrupole polarizability.} \end{aligned} \quad (2)$$

The self-consistent multipole moments of the ten (for kyanite) oxygen-ion sites were then calculated by simultaneous solution of the equations

TABLE I. Transformation matrices from crystallographic ( $a$ ,  $b$ ,  $c$ ) to orthogonal ( $x$ ,  $y$ ,  $z$ ) axes for kyanite, andalusite, and sillimanite.

	Kyanite			Andalusite and sillimanite		
	$a$	$b$	$c$	$a$	$b$	$c$
$x$	0.9418	0	0	1	0	0
$y$	-0.2757	1	0.0004	0	1	0
$z$	-0.1925	0	1.0000	0	0	1

TABLE II. Calculated and observed electric field gradients (nondiagonalized) in units of  $10^{14}$  esu.

		$\alpha_D = 1.1 \text{ \AA}^3, \alpha_Q = 0.1 \text{ \AA}^5, \gamma_\infty = -2.4$						
		$V_{xx}$	$V_{xy}$	$V_{xz}$	$V_{yy}$	$V_{yz}$	$V_{zz}$	$R$
Kyanite $V_{ij} \times (1 - \gamma_\infty)$								
Al (1)	calc	-3.528	+0.287	-0.388	+6.652	+3.624	-3.124	19%
	obs	-3.602	+0.269	-0.587	+8.443	+3.414	-4.841	
Al (2)	calc	+2.891	-0.089	-0.337	-1.407	-1.831	-1.484	62%
	obs	+2.837	-0.243	-0.996	-3.141	-0.951	+0.304	
Al (3)	calc	+4.230	+0.436	+0.705	-5.874	+2.584	+1.644	20%
	obs	+4.576	-0.049	+0.831	-5.714	+1.480	+1.138	
Al (4)	calc	+5.505	-0.530	+0.244	-8.578	+1.459	+3.073	7%
	obs	+5.933	-0.237	+0.195	-8.574	+1.292	+2.641	
Andalusite $V_{ij} \times (1 - \gamma_\infty)$								
Al (1)	calc	+8.405	+5.533	0	-1.304	0	-7.100	21%
	obs	+9.681	+8.803	0	-1.890	0	-7.791	
Al (2)	calc	-0.749	+0.444	0	-0.130	0	+0.879	82%
	obs	-1.113	+1.059	0	-4.349	0	+5.462	
Sillimanite $V_{ij} \times (1 - \gamma_\infty)$								
Al (1)	calc	-0.453	+2.768	-4.144	+4.681	+3.164	-4.228	21%
	obs	+0.860	+2.846	-4.319	+4.460	+1.934	-5.320	
Al (2)	calc	+0.698	+1.020	0	+3.641	0	-4.339	103%
	obs	-5.568	+2.699	0	+4.098	0	+1.470	

$$Q_r^s = \alpha_r \left( \sum_{s'=1}^{10} \sum_{r'=1}^9 K_r^{s s'} Q_{r'}^{s'} + V_r^s \right) \quad (3)$$

[for  $r=1-3$ ,  $\alpha_r = -\alpha_D(O^{2-})$ ; for  $r=4-9$ ,  $\alpha_r = -\alpha_Q(O^{2-})$ ;  $V_r^s$  is the potential coefficient due to monopoles]. These multipole moments were then used in Eq. (1) to find the field gradients at the four aluminum sites. These equations can be extended to include multipole moments of any order at every lattice site in the crystal. For each set of multipole polarizabilities, the ionic model gives the self-consistent potential distribution throughout the crystal, including, of course, the electric-field-gradient tensors at the Al<sup>27</sup> sites.

The lattice sums were evaluated by the Ewald<sup>22</sup> method, as extended by de Wette and Nijboer.<sup>23</sup> In this investigation, the summations were restricted to a volume of 125 unit cells, with a total of 4000 ions. To test the convergence, the point-charge fields and field gradients at all aluminum and oxygen sites in kyanite were calculated for 343 unit cells, which corresponds to 6976 additional ions. The change in the sums was greatest for the point-charge field at O<sub>c</sub>, and it was in the fifth significant figure.

The  $K$  factors were calculated by introducing point-charge clusters at the ionic sites to generate dipole and quadrupole lattices.<sup>12</sup> The dipoles consisted of a plus and minus charge separated by a

distance of 0.01 Å. The length of the linear quadrupoles was 0.04 Å, and the other quadrupoles were square, the length of the side being 0.02 Å. These are all quite small compared to the interatomic distances; the smallest Al-O distance is about 1.8 Å. This method was checked by varying the separations of the multipoles, and it was found that the potentials varied in the proper proportions.

#### IV. RESULTS

The nuclear-quadrupole coupling tensors of kyanite were measured by Hafner and Raymond,<sup>24</sup> those of andalusite were determined by Hafner, Raymond, and Ghose,<sup>25</sup> and the sillimanite tensors were measured by Raymond and Hafner.<sup>26</sup> The tensors are displayed in Tables II and III. The eight tensors are quite distinct, with a large spread (4–16 MHz) in the quadrupole coupling constants. In order to check our calculated tensors against experiment, it is of course necessary to make a correct assignment of each measured quadrupole coupling tensor to the correct Al site. The differences in the tensors must be attributed to distinct crystallographic properties of the corresponding sites. In sillimanite, Al(1) has point symmetry  $\bar{1}$  and so should have the maximum five field-gradient components, while Al(2), on a reflection plane, will have but three. This determines the assignment. However, as all four nonequivalent sites in kyanite have the same

TABLE III. Observed and calculated electric-field-gradient tensors (diagonalized). Parameters fitted individually for each crystal.

Kyanite									
Eigenvalues (MHz) ( $eQV_{ij}/h$ )									
Site	$V_{XX}$		$V_{YY}$		$V_{ZZ}$		$\eta$		Obs
	Calc <sup>a</sup>	Obs <sup>b</sup>	Calc	Obs	Calc	Obs	Calc	Obs	
Al (1)	-3.46	-3.70	-5.42	-6.32	8.88	10.01	0.22	0.26	
Al (2)	0.88	0.26	3.16	3.44	-4.04	-3.70	0.91	0.86	
Al (3)	1.68	1.35	4.78	5.16	-6.46	-6.51	0.48	0.59	
Al (4)	3.34	3.00	6.44	6.42	-9.77	-9.43	0.32	0.36	
Eigenvectors									
Site		Calc			Obs				
		X	Y	Z	X	Y	Z		
Al (1)	x	163°	85°	74°	164°	93°	75°		
	y	73°	107°	24°	74°	103°	21°		
	z	90°	18°	72°	89°	14°	76°		
Al (2)	x	85°	100°	40°	71°	106°	25°		
	y	174°	90°	84°	161°	91°	71°		
	z	86°	40°	50°	85°	16°	75°		
Al (3)	x	107°	72°	25°	104°	78°	18°		
	y	17°	84°	74°	14°	88°	76°		
	z	90°	161°	71°	91°	168°	78°		
Al (4)	x	94°	83°	8°	93°	83°	7°		
	y	4°	90°	86°	3°	91°	87°		
	z	91°	173°	83°	91°	173°	83°		
Andalusite									
Eigenvalues (MHz)									
Site	$V_{XX}$		$V_{YY}$		$V_{ZZ}$		$\eta$		Obs
	Calc <sup>c</sup>	Obs	Calc	Obs	Calc	Obs	Calc	Obs	
Al (1)	-6.69	-7.17	-8.80	-8.42	15.49	15.59	0.14	0.08	
Al (2)	-0.87	-0.86	-4.73	-5.04	5.60	5.90	0.69	0.71	
Eigenvectors									
Site		Calc			Obs				
		X	Y	Z	X	Y	Z		
Al (1)	x	63°	153°	90°	62°	152°	90°		
	y	90°	90°	0°	90°	90°	0°		
	z	27°	63°	90°	28°	62°	90°		
Al (2)	x	15°	75°	90°	17°	73°	90°		
	y	75°	165°	90°	73°	163°	90°		
	z	90°	90°	0°	90°	90°	0°		
Sillimanite									
Eigenvalues (MHz)									
Site	$V_{XX}$		$V_{YY}$		$V_{ZZ}$		$\eta$		Obs
	Calc <sup>d</sup>	Obs	Calc	Obs	Calc	Obs	Calc	Obs	
Al (1)	3.43	2.40	5.82	6.53	-9.25	-8.93	0.26	0.46	
Al (2)	0.90	1.59	4.09	5.19	-4.99	-6.77	0.64	0.53	

TABLE III. (Continued)

Site		Eigenvectors					
		X	Calc Y	Z	X	Obs Y	Z
Al (1)	<i>x</i>	145°	69°	64°	136°	63	58°
	<i>y</i>	114°	156°	91°	121°	149°	87°
	<i>z</i>	66°	101°	27°	62°	104°	32°
Al (2)	<i>x</i>	90°	90°	0°	90°	90°	0°
	<i>y</i>	111°	21°	90°	105°	15°	90°
	<i>z</i>	21°	69°	90°	15°	75°	90°

<sup>a</sup>  $\alpha_D = 0.7 \text{ \AA}^3$ ,  $\alpha_Q = 0.1 \text{ \AA}^5$ ,  $\gamma_\infty = -4.0$ ,  $R = 19\%$ .

<sup>b</sup> Refined values, obtained by diagonalization of the Hamiltonian matrix for the mixed magnetic and

electrostatic interaction (see Ref. 25).

<sup>c</sup>  $\alpha_D = 0.5 \text{ \AA}^3$ ,  $\alpha_Q = 0.0 \text{ \AA}^5$ ,  $\gamma_\infty = -6.4$ ,  $R = 6\%$ .

<sup>d</sup>  $\alpha_D = 0.5 \text{ \AA}^3$ ,  $\alpha_Q = 0.1 \text{ \AA}^5$ ,  $\gamma_\infty = -4.0$ ,  $R = 21\%$ .

point symmetry (1), the tensors cannot be assigned on this basis. In andalusite, the different symmetries of the two nonequivalent sites have the same effect on the tensors; i. e., one of the principal axes of each site must be parallel to the *c* axis. As was pointed out in an earlier paper,<sup>24</sup> the sum over point charges alone does not enable an assignment to be made in the kyanite crystal. In andalusite, comparison of the point-charge eigenvectors makes the assignment Al(1)=Al(I) and Al(2)=Al(II) very likely. [Roman numerals refer to experimental values, numbered in order of the magnitude of  $eQV_{zz}/h$ , the largest being Al(I).] Higher moments must be included before attempting any further assignments.

For each set of multipole polarizabilities, a set of ionic field gradients can be calculated self-consistently. By suitably adjusting these polarizabilities, and also *Q* and  $\gamma_\infty$  of the Al<sup>3+</sup> ions, the theoretical field gradients that give the best fit to the measured data can be found. It is sensible to make some simplifying approximations at this point. First, only monopole, dipole, and quadrupole terms are included in the multipole series. This will be justified later on. Second, only monopole terms are included for the Al<sup>3+</sup> and Si<sup>4+</sup> ions. Theoretical calculations<sup>27</sup> of the polarizabilities of Al<sup>3+</sup> and Si<sup>4+</sup> free ions give  $\alpha_D(\text{Al}^{3+}) = 0.05 \text{ \AA}^3$ ,  $\alpha_Q(\text{Al}^{3+}) = 0.009 \text{ \AA}^5$ ,  $\alpha_D(\text{Si}^{4+}) = 0.03 \text{ \AA}^3$ , and  $\alpha_Q(\text{Si}^{4+}) = 0.004 \text{ \AA}^5$ . These are considerably smaller than the oxygen-ion polarizabilities, which we shall find to be  $\alpha_D(\text{O}^{2-}) \sim 1 \text{ \AA}^3$ ,  $\alpha_Q(\text{O}^{2-}) \sim 0.1 \text{ \AA}^5$ . The nuclear-quadrupole moment of Al<sup>27</sup> has been measured<sup>28</sup> as  $0.149 \times 10^{-24} \text{ cm}^2$ . This leaves  $\alpha_D(\text{O}^{2-})$ ,  $\alpha_Q(\text{O}^{2-})$ , and  $\gamma_\infty(\text{Al}^{3+})$  as variable parameters. Tessman, Kahn, and Shockley<sup>29</sup> report a range of values 0.5–3.2  $\text{ \AA}^3$  for  $\alpha_D(\text{O}^{2-})$  in quite a number of ionic crystals. The oxygen-ion polarizability in aluminum silicates should be within this range. Theoretical calculations of the Sternheimer factor for the Al<sup>3+</sup> free ion yield a value around –2.5.<sup>27,30–33</sup> The quadrupole polarizability of oxygen has been shown<sup>12</sup> to be less than 1.0  $\text{ \AA}^5$  in Al<sub>2</sub>O<sub>3</sub> although theoretical values<sup>27,32</sup> are far higher.

With the above values serving as guides, the 20 field-gradient components of kyanite, the eight field-gradient components of sillimanite, and the six field-gradient components of andalusite were calculated as functions of  $\alpha_D(\text{O}^{2-})$ ,  $\alpha_Q(\text{O}^{2-})$ , and  $\gamma_\infty(\text{Al}^{3+})$ . Before deciding which polarizabilities give the best fit, the measured field-gradient tensors must first be assigned to the correct sites. For andalusite, the tentative assignment Al(1)=Al(I), based on the monopole lattice sum, is confirmed. The calculated coupling constant for Al(1) is much larger than that of Al(2), as is the case for the observed ones (see Tables II and III). The point-charge eigenvectors were in very good agreement with experiment. The introduction of polarizabilities of the oxygen ion has very little effect on the eigenvectors, so they maintain their agreement.

The assignment is more difficult in kyanite, where it can be made in 24 different ways. For all reasonable polarizabilities, one site [Al(2)], has a much smaller calculated coupling constant than the rest. Al(IV) is assigned to this site. The field gradients at Al(3) are always second smallest, so Al(III) is assigned to this site. Al(I) and Al(II) have nearly the same coupling constants, so the assignment must be made on the basis of the eigenvectors. Here we assign Al(1) to Al(I) and Al(4) to Al(II). Tables II and III show the calculated and observed field-gradient tensors for two different sets of polarizabilities and Sternheimer factors, both of which give very good fits. The assignment is clearly correct for these polarizabilities; any assignment change would make the fit much worse.

The next problem is to find the polarizabilities which give the best fit to the observed data. To this end, disagreement indices *R* were computed for all sets of polarizabilities and Sternheimer factors used:

$$R = \frac{\sum |V_{ij}^{\text{obs}} - V_{ij}^{\text{calc}}|}{\sum |V_{ij}^{\text{obs}}|} \quad (4)$$

The sum is over the field-gradient components at

TABLE IV. Combinations of parameters for fitting the ionic model to observed quadrupole coupling data. Percentage disagreements ( $R$ ).

$\alpha_D(O^{2-})[\text{\AA}^3]$	$\alpha_Q(O^{2-})[\text{\AA}^5]$	$\gamma_\infty(\text{Al}^{3+})$	All sites	Kyanite		Sillimanite		Andalusite	
				Al(1), Al(2), Al(3), Al(4)	Al(1)	Al(2)	Al(1)	Al(2)	
0.4	0.1	-5.3	25	22	39	27	17	29	
0.5	0.1	-4.9	21	20	30	24	15	26	
0.6	0.1	-4.5	22	19	25	35	14	35	
0.7	0.1	-4.0	23	19	19	50	14	46	
0.8	0.1	-3.6	25	19	16	66	14	56	
0.9	0.1	-3.2	27	19	13	81	15	63	
1.0	0.1	-2.7	32	20	18	90	19	74	
1.1	0.1	-2.4	34	21	21	103	21	82	
1.2	0.1	-2.1	37	23	23	112	23	89	
1.3	0.1	-1.9	39	24	25	120	23	97	
1.4	0.1	-1.7	42	25	28	127	23	101	
1.5	0.1	-1.5	42	25	32	122	24	104	

the Al sites in question. The  $R$  indices were computed for all possible site assignments in each crystal. A number of disagreement indices must be computed for each set of parameters, and each assignment, in order to resolve the ambiguities in the signs of the measured field gradients. There is an over-all ambiguity at all sites, and further ambiguities in the signs of the off-diagonal elements in andalusite and sillimanite. The disagreement was small enough to resolve these ambiguities, and confirm the assignments.

It was found that the smallest  $R$  index, 21%, was obtained with  $\alpha_D = 0.5 \text{\AA}^3$ ,  $\alpha_Q = 0.1 \text{\AA}^5$ , and  $\gamma_\infty = -4.9$ . The best fit in kyanite alone,  $R = 19\%$ , was with  $\alpha_D = 0.7 \text{\AA}^3$ ,  $\alpha_Q = 0.1 \text{\AA}^5$ ,  $\gamma_\infty = -4.0$ . For sillimanite, the best fit was  $R = 21\%$ ,  $\alpha_D = 0.5 \text{\AA}^3$ ,  $\alpha_Q = 0.1 \text{\AA}^5$ ,  $\gamma_\infty = -4.0$ ; and in andalusite, with  $\alpha_D = 0.5 \text{\AA}^3$ ,  $\alpha_Q = 0.0 \text{\AA}^5$ , and  $\gamma_\infty = -6.4$ ,  $R = 6\%$ . The observed and calculated tensors using these parameters are given in Table III. The parameters can be varied about these values without increasing the disagreement a great deal. The quadrupole polarizability of the oxygen ion,  $\alpha_Q(O^{2-})$  can be determined most easily. For  $\alpha_Q = 0$ , the smallest  $R$  is 25% for  $\alpha_D = 0.5 \text{\AA}^3$  and  $\gamma_\infty = -5.4$ . For  $\alpha_Q = 0.2 \text{\AA}^5$  the smallest  $R$  is 31% for  $\alpha_D = 0.6 \text{\AA}^3$  and  $\gamma_\infty = -3.6$ . Values of  $\alpha_Q$  in the range  $0-0.1 \text{\AA}^5$  fit about equally well, but above this the fit becomes worse.  $\alpha_D$  and  $\gamma_\infty$  are more difficult to pin down. This is shown in Table IV. For each  $\alpha_D(O^{2-})$  listed, the  $\gamma_\infty$  that gives the best fit and the corresponding  $R$  index are shown. While  $R$  increases with  $\alpha_D$  above  $0.5 \text{\AA}^3$ , this is due almost entirely to Al(2) in andalusite, which is five-coordinated, and Al(2) in sillimanite, which is tetrahedral. At the octahedral sites, values of  $\alpha_D$  between  $0.7$  and  $1.1 \text{\AA}^3$ , with  $\gamma_\infty = -4.0$  to  $-2.4$ , give about equally good fits. If we had no further information about  $\alpha_D$ ,  $\alpha_Q$ , and  $\gamma_\infty$ , and treated them strictly as variable parameters, then our results would be  $\alpha_D = 0.5-0.7 \text{\AA}^3$ ,  $\gamma_\infty = -4.0$  to  $-6.4$ , and  $\alpha_Q = 0.0-0.2 \text{\AA}^5$ . If only octahedral sites

are considered, then the parameters would be  $\alpha_D = 0.4-1.5 \text{\AA}^3$ ,  $\gamma_\infty = -5.3$  to  $-1.5$ , and  $\alpha_Q = 0.0-0.2 \text{\AA}^5$ . The best fit at these sites is at  $\alpha_D = 0.9 \text{\AA}^3$ ,  $\alpha_Q = 0.1 \text{\AA}^5$ ,  $\gamma_\infty = -3.2$ .

In Fig. 1, an example is given of the dependence of the calculated quadrupole coupling constant on the polarizabilities  $\alpha_D$  and  $\alpha_Q$  of oxygen. In Fig. 2, the dependence of the eigenvectors on oxygen polarizability is shown.

## V. DISCUSSION

The polarizabilities and Sternheimer factor found using the variable-parameter approach can be compared with values derived by other methods. Dipole polarizabilities can be obtained from refractive index data, using a Lorentz factor of  $\frac{4}{3}\pi$ , which is strictly valid only for cubic crystals.<sup>29</sup> The re-

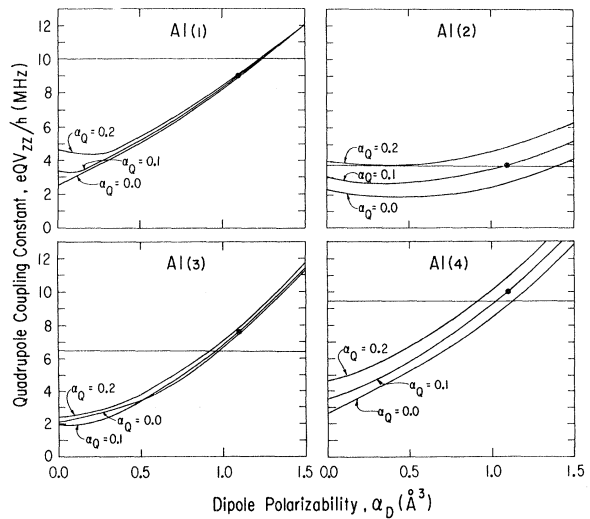


FIG. 1. Plot of the quadrupole coupling constants in kyanite vs the oxygen-ion dipolar polarizability.  $\alpha_Q$  is the quadrupolar polarizability. Horizontal line is the measured value. Large dot represents  $\alpha_D = 1.1 \text{\AA}^3$ ,  $\alpha_Q = 0.1 \text{\AA}^5$ . Sternheimer factor = -2.6.

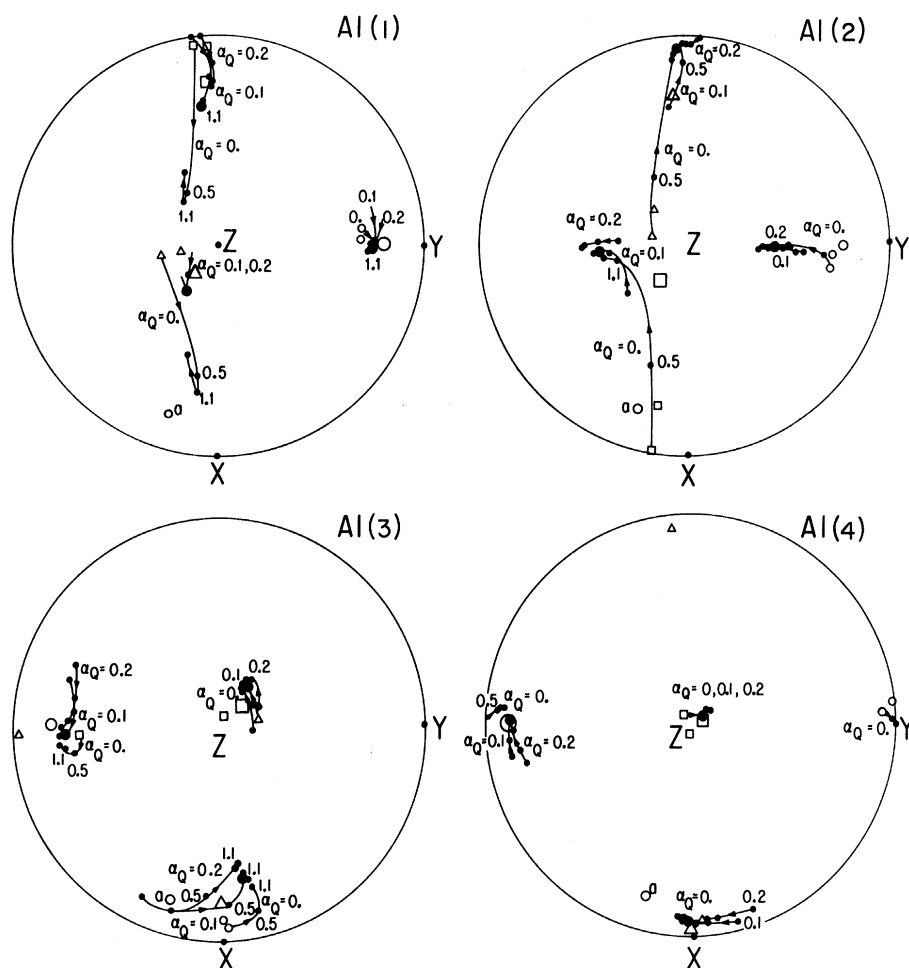


FIG. 2. Stereographic projection of the observed and calculated eigenvectors of the kyanite electric-field-gradient tensors. Large open symbols are the observed vectors. Circles:  $V_{ZZ}$ ; triangles:  $V_{YY}$ ; squares:  $V_{XX}$ . Small open symbols are the point-charge values. There are two sets of these, for Burnham (Ref. 15) and de Rango (Ref. 16) coordinates. Lines with arrows show the movement of the eigenvectors as  $\alpha_D(O^{2-})$  is increased from 0 to  $1.5 \text{ \AA}^3$ . There are three sets of lines, for  $\alpha_Q = 0, 0.1, 0.2 \text{ \AA}^5$ . There are dots on the lines at  $\alpha_D = 0.5, 1.1,$  and  $1.5 \text{ \AA}^3$ . Large dot is  $\alpha_D = 1.1 \text{ \AA}^3, \alpha_Q = 0.1 \text{ \AA}^5$ .

fractive anisotropy is small in these crystals, the indices ranging from 1.63 to 1.65 in andalusite, 1.65 to 1.67 in sillimanite, and 1.71 to 1.73 in kyanite.<sup>34</sup> This procedure gives polarizabilities  $\alpha_D(O^{2-}) = 1.36 \text{ \AA}^3$  for kyanite,  $\alpha_D(O^{2-}) = 1.44 \text{ \AA}^3$  for sillimanite, and  $\alpha_D(O^{2-}) = 1.45 \text{ \AA}^3$  for andalusite. The same procedure gives  $1.34 \text{ \AA}^3$  for corundum ( $\alpha\text{-Al}_2\text{O}_3$ ).<sup>29</sup>

Theoretical calculations of the oxygen-ion dipole and quadrupole polarizability, and the aluminum-ion Sternheimer factor, have been performed. For the dipole polarizability, the calculated values  $\alpha_D(O^{2-})$  range from 3 to  $134 \text{ \AA}^3$ . For  $\alpha_D(O^{2-})$ , the values are 7–1000  $\text{ \AA}^5$ , for  $\gamma_\infty(\text{Al}^{3+})$ , the range is  $-2.24$  to  $-2.74$ . A summary of these results is given in Table V. The polarizability results do not agree at all. The Sternheimer factors do agree rather well. However,  $\text{Al}^{27}$  in kyanite is not necessarily the same as the free  $\text{Al}^{3+}$  ion. Lahiri and Mukherji<sup>32,36</sup> have devised an interpolation relation for ions in crystals, based on changes in the electron-density distribution. The radius of maximum electron density,  $\rho_m$ , for the ion in the crystal is required. This was derived from electron-density maps of kyanite

supplied by Burnham. Averaged over the four sites and corrected for thermal vibrations, this radius is  $0.305 \pm 0.020 \text{ \AA}$ . For the free  $\text{Al}^{3+}$  ion,  $\rho_m = 0.239 \text{ \AA}$ .<sup>32</sup> Using the interpolation relation,<sup>36</sup>  $\gamma_\infty$  for  $\text{Al}^{3+}$  in kyanite is found to be  $-5.6 \pm 1.5$ . The spreading out of the ion results in a much larger  $\gamma_\infty$ .

None of the above calculations give a definite value for either  $\alpha_D(O^{2-})$ ,  $\alpha_Q(O^{2-})$ , or  $\gamma_\infty$  of  $\text{Al}^{3+}$ . The refractive-index calculations, together with Tessman, Kahn, and Shockley's<sup>29</sup> lists of  $O^{2-}$  polariz-

TABLE V. Theoretical values of  $\alpha_D(O^{2-})$ ,  $\alpha_Q(O^{2-})$ , and  $\gamma_\infty(\text{Al}^{3+})$ .

$\alpha_D(O^{2-}) (\text{ \AA}^3)$		$\alpha_Q(O^{2-}) (\text{ \AA}^5)$		$\gamma_\infty(\text{Al}^{3+})$	
Value	Ref.	Value	Ref.	Value	Ref.
$\sim 2.8$	35	$\sim 7$	35	$-2.24$	27
10.56	32	412.5	32	$-2.34$	31
65.88	27	399.8	27	$-2.46$	33
134.3	27	1044.	27	$-2.57$	32
				$-2.59$	30
				$-2.74$	31

TABLE VI. Comparison of point-charge field gradients, Burnham and de Rango parameters.

		Field gradients ( $10^{14}$ esu)					
		$V_{xx}$	$V_{yy}$	$V_{zz}$	$V_{xy}$	$V_{xz}$	$V_{yz}$
Al (1)	Burnham	-0.083	+0.496	-0.414	-0.053	-0.065	+0.395
	de Rango	-0.011	+0.500	-0.489	-0.010	-0.051	+0.431
Al (2)	Burnham	+0.090	+0.464	+0.374	-0.102	-0.058	-0.315
	de Rango	+0.168	-0.498	+0.330	-0.038	-0.106	-0.319
Al (3)	Burnham	+0.540	-0.235	-0.305	+0.023	+0.062	-0.033
	de Rango	+0.509	-0.336	-0.173	-0.004	+0.079	+0.006
Al (4)	Burnham	+0.636	-0.680	+0.043	+0.058	+0.048	-0.049
	de Rango	+0.603	-0.695	+0.092	+0.108	-0.039	-0.011

abilities in various compounds, indicate an  $\alpha_D(O^{2-})$  in the range of 1.0 to 1.5  $\text{\AA}^3$  for our crystals. These polarizabilities give the best fit to the observed data with Sternheimer factors of -2.7 to -1.5 and  $\alpha_Q(O^{2-})=0.01 \text{\AA}^5$ . These Sternheimer factors are reasonable with respect to the theoretical values for the free ion. Our best set of parameters for all eight sites is  $\alpha_D=0.5 \text{\AA}^3$ ,  $\alpha_Q=0.1 \text{\AA}^5$ ,  $\gamma_\infty=-4.9$ . This dipole polarizability is rather smaller than expected, and  $\gamma_\infty$  larger, although it does agree with the interpolation relation.<sup>32,36</sup> If the octahedral sites alone are considered, the fit obtained using theoretical values  $\alpha_D=1.1 \text{\AA}^3$ ,  $\gamma_\infty=-2.4$ ,  $R(\text{octahedral})=21\%$  is nearly as good as the best fit (Table IV). In Table II is a comparison of the observed and calculated field gradients using  $\alpha_D=1.1 \text{\AA}^3$ ,  $\gamma_\infty=-2.4$ , and  $\alpha_Q=0.1 \text{\AA}^5$ . The agreement at the six octahedral sites is good; at the tetrahedral and five-coordinated sites, not so good. Al(2) in kyanite is the worst-fitting octahedral site. However, the over-all agreement is better than in most previous field-gradient calculations.

One possible source of error is the crystal structure determination. For kyanite, there are two recent refinements, those of Burnham<sup>15</sup> and of de Rango *et al.*<sup>16</sup> Burnham's<sup>15</sup> coordinates were used for the complete calculation. The point-charge lattice sums only were calculated using de Rango's<sup>16</sup> coordinates. A comparison of the results is shown in Table VI. The point-charge eigenvectors obtained using both coordinate sets are shown in Fig. 2. In addition, the complete calculation of the field gradients in kyanite was done using Burnham  $K$  factors and de Rango point-charge values. (The  $K$  factors are less sensitive to small coordinate changes than point-charge values.) Using the polarizability values  $\alpha_D=1.0 \text{\AA}^3$ ,  $\alpha_Q=0$ , the disagreement between the two calculations is 8% at Al(1), 17% at Al(2), 6% at Al(3), and 5% at Al(4). The coordinates of the Al(2) octahedra do not differ between the two refinements more than the other octahedra. The greater sensitivity of the Al(2) field gradients to the coordinates may partly explain the poorer fit at Al(2).

The thermal motion of the ions causes effective quadrupole moments at the lattice sites. These will also produce field gradients. The anisotropic temperature factors of Burnham<sup>15,19,21</sup> were used to calculate these quadrupole moments and the resulting field gradients. No great accuracy is claimed for these temperature factors, but the results, shown in Table VII, should be of the right order of magnitude. On the average, their contribution is about 15% of that of the static quadrupoles (see Table VIII). They have the largest effect at Al(3) in kyanite, about 30% of the static quadrupole contribution, and 5% of the total field gradient.

The neglect of multipole moments at the Al and Si sites also introduces error into our calculated field gradients. The polarizabilities<sup>27,33</sup> of  $\text{Al}^{3+}$  and  $\text{Si}^{4+}$  are only about 5% of the oxygen values, so the error should be of this order of magnitude.

The effect of induced octupole moments could also be considered. There are no reliable calculations of the octupole polarizability, but it could be entered as another variable parameter. The contribution of induced octupoles was considered<sup>13</sup> for the case of corundum ( $\alpha\text{-Al}_2\text{O}_3$ ), but no conclusions could be drawn as to its magnitude. The quadrupole contribution to the field gradients is less than 25% of the

TABLE VII. External field gradients due to thermal motion of the ions in units of  $10^{14}$  esu.

	$V_{xx}$	$V_{yy}$	$V_{zz}$	$V_{xy}$	$V_{xz}$	$V_{yz}$
Kyanite						
Al (1)	-0.018	+0.002	+0.016	+0.039	-0.009	0.000
Al (2)	-0.005	-0.036	+0.041	+0.006	-0.004	+0.032
Al (3)	+0.074	-0.078	+0.004	+0.013	+0.004	+0.028
Al (4)	-0.016	-0.010	+0.026	+0.025	+0.008	+0.016
Andalusite						
Al (1)	-0.015	+0.035	-0.020	-0.008	0	0
Al (2)	+0.026	-0.023	-0.003	-0.011	0	0
Sillimanite						
Al (1)	+0.016	+0.025	-0.041	+0.018	+0.004	+0.025
Al (2)	-0.002	+0.021	-0.019	+0.053	0	0



TABLE VIII. Dipole and quadrupole moments and contributions to field gradients.

$\alpha_D = 1.1 \text{ \AA}^3, \alpha_Q = 0.1 \text{ \AA}^5$									
Quadrupole moments ( $10^{-26} \text{ cm}^2$ )						Dipole moments ( $10^{-18} \text{ cm}$ )			
	$Q_{xx}$	$Q_{yy}$	$Q_{zz}$	$Q_{xy}$	$Q_{xz}$	$Q_{yz}$	$D_x$	$D_y$	$D_z$
$O_a^a$	-0.055	-0.401	+0.464	-0.599	-0.237	-0.004	-2.451	-0.319	+0.611
$O_b$	+0.036	+0.010	-0.048	+0.168	+0.188	+0.041	-1.759	-2.288	-1.012
$O_c$	+0.546	-0.223	-0.325	-0.006	-0.334	+0.524	+0.759	+0.691	-2.304
$O_d$	+0.536	-0.241	-0.295	+0.051	+0.313	+0.545	+0.993	-0.676	+2.180
$O_e$	-0.180	-0.309	+0.487	+0.566	+0.257	+0.029	-2.186	+0.521	-1.050
$O_f$	-0.012	+0.090	-0.078	-0.084	-0.224	+0.075	-1.565	+1.990	+0.938
$O_g$	+0.417	-0.077	-0.355	-0.062	+0.309	-0.489	+1.110	+1.146	+2.364
$O_h$	+0.439	-0.073	-0.362	+0.053	-0.287	+0.506	+1.268	-1.329	-2.429
$O_k$	-0.468	+0.353	+0.115	+0.506	-0.051	+0.020	+0.717	-2.141	-0.386
$O_m$	-0.457	+0.342	+0.117	-0.540	+0.045	+0.022	+0.817	+2.292	+0.359
$O_a$	+0.401	-0.301	-0.100	-0.289	0	0	-2.077	-0.350	0
$O_b$	-0.179	+0.039	+0.140	-0.638	0	0	+2.154	-0.360	0
$O_c$	-0.339	-0.337	+0.676	+0.399	0	0	-0.693	+1.287	0
$O_d$	+0.194	+0.229	-0.423	-0.202	-0.183	+0.492	-0.941	-2.167	+1.486
$O_a$	-0.666	+0.550	+0.115	-0.482	0	0	+2.588	-0.106	0
$O_b$	-0.269	+0.333	-0.064	-0.399	0	0	+0.367	+0.932	0
$O_c$	-0.156	-0.490	+0.646	-0.995	0	0	+0.760	+2.044	0
$O_d$	+0.579	-0.085	-0.494	-0.298	-0.091	-0.215	+0.227	-2.285	-1.058
Kyanite									
Field gradients ( $10^{14} \text{ esu}$ )									
		$V_{xx}$	$V_{yy}$	$V_{zz}$	$V_{xy}$	$V_{xz}$	$V_{yz}$		
A1(1)	Point charge	-0.083	+0.496	-0.414	-0.053	-0.066	+0.395		
	Dipole	-1.160	+1.398	-0.238	+0.144	-0.043	+0.651		
	Quadrupole	+0.204	+0.066	-0.270	-0.007	-0.005	+0.021		
	Total	-1.039	+1.960	-0.922	+0.084	-0.114	+1.067		
A1(2)	Point charge	+0.090	-0.464	+0.374	-0.102	-0.058	-0.315		
	Dipole	+0.503	+0.067	-0.569	+0.109	-0.021	-0.036		
	Quadrupole	+0.258	-0.018	-0.241	-0.034	-0.021	-0.187		
	Total	+0.851	-0.415	-0.436	-0.027	-0.100	-0.538		
A1(3)	Point charge	+0.540	-0.235	-0.305	+0.023	+0.062	-0.034		
	Dipole	+0.835	-1.449	+0.614	+0.371	+0.128	+0.727		
	Quadrupole	-0.131	-0.043	+0.174	-0.265	+0.018	+0.067		
	Total	+1.244	-1.727	+0.483	+0.129	+0.208	+0.760		
A1(4)	Point charge	+0.636	-0.680	+0.043	+0.058	+0.048	-0.048		
	Dipole	+0.921	-1.673	+0.753	-0.507	+0.058	+0.283		
	Quadrupole	+0.059	-0.159	+0.100	+0.293	-0.039	+0.193		
	Total	+1.616	-2.512	+0.896	-0.156	+0.067	+0.428		
Andalusite									
A1(1)	Point charge	+0.926	+0.002	-0.928	+0.739	0	0		
	Dipole	+1.327	-0.540	-0.787	+0.829	0	0		
	Quadrupole	+0.219	+0.155	-0.374	+0.059	0	0		
	Total	+2.472	-0.383	-2.089	+1.627				
A1(2)	Point charge	-0.397	-0.896	+1.293	+0.166	0	0		
	Dipole	+0.369	+0.853	-1.223	-0.371	0	0		
	Quadrupole	-0.193	+0.005	+0.188	+0.075	0	0		
	Total	-0.221	-0.038	+0.258	-0.130				

TABLE VIII. (Continued)

		Sillimanite					
		$V_{xx}$	$V_{yy}$	$V_{zz}$	$V_{xy}$	$V_{xz}$	$V_{yz}$
Al(1)	Point charge	+0.615	+0.406	-1.021	-0.089	-0.666	-0.063
	Dipole	-0.878	+0.793	+0.085	+1.024	-0.524	+1.147
	Quadrupole	+0.129	+0.179	-0.308	-0.121	-0.029	-0.154
	Total	-0.134	+1.378	-1.244	+0.814	-1.219	+0.930
Al(2)	Point charge	-1.100	+0.033	+1.067	+0.475	0	0
	Dipole	+1.490	+1.182	-2.672	-0.493	0	0
	Quadrupole	-0.185	-0.144	+0.329	+0.318	0	0
	Total	+0.205	+1.071	-1.276	+0.300		

<sup>a</sup>The atom notation of Refs. 15-21 is used here.  $O_a-O_m$  are the kyanite oxygen positions. The first  $O_a-O_d$  are andalusite, second are sillimanite.

dipole contribution at five of the six sites. The exception is Al(2) in kyanite; here it is 60%. We would expect the octupole contribution to be small then, with the possible exception of site Al(2).

Depending on the choice of polarizabilities, the disagreement between calculated and observed values is about 20-30% at Al(1) in kyanite, 40-70% at Al(2), 20-30% at Al(3), and 10-20% at Al(4). In andalusite, the disagreement is 10-20% at Al(1) and 10-100% at Al(2). In sillimanite, the disagreement is 10-40% at Al(1) and 25-120% at Al(2).

The ionic model is not expected to give perfect field gradients in the silicates, which are not completely ionic crystals. The disagreement gives an indication of the amount of nonionic effects, such as covalent bonding, at each site. This disagreement is small at all the sites except the Al(2) site in each crystal. It is about 20%, and most of this could be accounted for by the errors and approximations discussed above. Al(2) in kyanite is the only site where the quadrupole contribution is nearly as large as the dipole contribution to the field gradients, so the large disagreement here could be due to the effects of induced octupoles. The ionic model appears to fail only at the five-coordinated site Al(2) in andalusite, and the tetrahedral Al(2) in sillimanite. Even at these sites it may be acceptable, if the theoretical  $\alpha_D(O^{2-})$  and  $\gamma_\infty(Al^{3+})$  are either incorrect or very greatly modified by the crystalline environment (see Table IV). The average Al-O distance at the andalusite site is 1.836 Å,<sup>19</sup> and at the sillimanite site 1.760 Å,<sup>21</sup> compared with<sup>15,19</sup> 1.897-1.935 at the

octahedral sites. Overlapping of the ions may make the ionic model inadequate.

It has been pointed out that analysis of the charge distribution in terms of point multipoles may be inaccurate, and that the extended nature of the actual induced moments must be taken into account.<sup>37</sup> The size of the actual induced moments can be calculated from the values in Table VIII. The oxygen-dipole moments do not exceed  $3 \times 10^{-18}$  cm, corresponding to a separation of  $\sim 0.3$  Å. The quadrupole moments are not larger than  $1.5 \times 10^{-26}$  cm<sup>2</sup>, a separation of  $\sim 0.4$  Å. The Al-O distance is  $\sim 1.8$  Å; therefore, it is to be expected that the extended nature of the moments would have an effect on the field gradients, but not a large one.

The effects of covalent bonding have been introduced into our calculations only in a very limited way. Our polarizabilities are not free-ion polarizabilities, but best-fit values, and there is probably some covalent contribution to them.<sup>38</sup> Covalent effects could be calculated more explicitly, by modifying the charge distribution. Phillips<sup>39</sup> has suggested a two-part covalent charge distribution, one part centered at atomic sites, and the other at covalent sites. It would be interesting to adapt this model to treat electric field gradients.

#### ACKNOWLEDGMENT

The author wishes to express his appreciation to his thesis advisor, Professor S. S. Hafner, who suggested this study and provided sponsorship and guidance for the research.

<sup>†</sup>Work supported by the National Science Foundation, Grant No. GA-1134, and an ARPA contract at The University of Chicago.

\*Thesis submitted to the Department of Physics of The University of Chicago in partial fulfillment of the requirements for the Ph. D. degree.

<sup>‡</sup>Present address: Carnegie Institution at Washington, Geophysical Laboratory, Washington, D. C. 20008.

<sup>1</sup>R. Bersohn, J. Chem. Phys. **29**, 326 (1958).

<sup>2</sup>E. Brun and S. Hafner, Z. Krist. **117**, 63 (1962).

<sup>3</sup>T. T. Taylor and T. P. Das, Phys. Rev. **133**, A1327 (1964).

<sup>4</sup>S. S. Hafner and P. Hartmann, Helv. Phys. Acta **37**, 348 (1964).

<sup>5</sup>R. R. Sharma and T. P. Das, J. Chem. Phys. **41**, 3581 (1964).

<sup>6</sup>J. O. Artman and J. C. Murphy, Phys. Rev. **135**, A1622 (1964).

<sup>7</sup>J. O. Artman, Phys. Rev. **143**, 541 (1966).

<sup>8</sup>C. A. Sholl, Proc. Phys. Soc. (London) **87**, 897

- (1966).
- <sup>9</sup>L. D. V. Rao and D. V. G. L. N. Rao, *Phys. Rev.* **160**, 274 (1967).
- <sup>10</sup>D. Schwarzenbach, *Z. Krist.* **123**, 422 (1966).
- <sup>11</sup>R. M. Sternheimer, *Phys. Rev.* **84**, 244 (1951); H. M. Foley, R. M. Sternheimer, and D. Tycko, *ibid.* **93**, 734 (1954); R. M. Sternheimer and H. M. Foley, *ibid.* **102**, 731 (1956).
- <sup>12</sup>S. S. Hafner and M. Raymond, *Solid State Commun.* **5**, 833 (1967); S. S. Hafner and M. Raymond, *J. Chem. Phys.* **49**, 3570 (1968).
- <sup>13</sup>S. S. Hafner and M. Raymond, *J. Chem. Phys.* **52**, 279 (1970).
- <sup>14</sup>M. Raymond and S. S. Hafner, *Phys. Rev.* **B1**, 979 (1970).
- <sup>15</sup>C. W. Burnham, *Z. Krist.* **118**, 337 (1963).
- <sup>16</sup>C. de Rango, G. Isoucaris, C. Zelwer, and J. Devaux, *Bull. Soc. Franc. Mineral. Crist.* **89**, 419 (1966).
- <sup>17</sup>S. Naray-Szabo, W. H. Taylor, and W. W. Jackson, *Z. Krist.* **71**, 117 (1929).
- <sup>18</sup>W. H. Taylor, *Z. Krist.* **71**, 205 (1929).
- <sup>19</sup>C. W. Burnham and M. J. Buerger, *Z. Krist.* **115**, 269 (1961).
- <sup>20</sup>W. H. Taylor, *Z. Krist.* **68**, 503 (1928).
- <sup>21</sup>C. W. Burnham, *Z. Krist.* **118**, 127 (1963).
- <sup>22</sup>P. O. Ewald, *Ann. Physik* **64**, 253 (1921).
- <sup>23</sup>F. W. de Wette and B. R. Nijboer, *Physica* **24**, 1105 (1958).
- <sup>24</sup>S. S. Hafner and M. Raymond, *Am. Mineralogist* **52**, 1632 (1967).
- <sup>25</sup>S. S. Hafner, M. Raymond, and S. Ghose, *J. Chem. Phys.* **52**, 6037 (1970).
- <sup>26</sup>M. Raymond and S. S. Hafner, *J. Chem. Phys.* **53**, 4110 (1970).
- <sup>27</sup>P. W. Langhoff and R. P. Hurst, *Phys. Rev.* **139**, A1415 (1965).
- <sup>28</sup>H. Lew and G. Wessel, *Phys. Rev.* **90**, 1 (1953).
- <sup>29</sup>J. R. Tessman, A. H. Kahn, and W. Shockley, *Phys. Rev.* **92**, 890 (1953).
- <sup>30</sup>T. P. Das and R. Bersohn, *Phys. Rev.* **102**, 733 (1956).
- <sup>31</sup>Gerald Burns, *J. Chem. Phys.* **31**, 1253 (1959).
- <sup>32</sup>J. Lahiri and A. Mukherji, *Phys. Rev.* **153**, 386 (1967).
- <sup>33</sup>F. D. Feiock and W. R. Johnson, *Phys. Rev.* **187**, 39 (1969).
- <sup>34</sup>W. A. Deer, R. A. Howie, and J. Zussman, *Rock-Forming Minerals* (Longmans, Green, and Co., London, 1962), Vol. I, pp. 129, 137.
- <sup>35</sup>G. Burns and E. G. Wikner, *Phys. Rev.* **121**, 155 (1961).
- <sup>36</sup>J. Lahiri and A. Mukherji, *Proc. Phys. Soc. (London)* **87**, 913 (1966).
- <sup>37</sup>G. Burns, *J. Chem. Phys.* **42**, 377 (1965).
- <sup>38</sup>M. Tachiki and Z. Sroubek, *J. Chem. Phys.* **48**, 2383 (1968).
- <sup>39</sup>J. C. Phillips, *Phys. Rev.* **166**, 832 (1968); *Covalent Bonding in Crystals, Molecules, and Polymers* (University of Chicago, Chicago, 1969), pp. 67-74.

## Emission of Charged Particles from Crystals

A. P. Pathak and M. Yussouff

*Department of Physics, Indian Institute of Technology, Kanpur-16, U. P., India*

(Received 17 September 1970)

A quantum-mechanical treatment of the problem of the charged-particle emission from crystals has been presented. In addition to the mass and potential dependence established by the previous wave-mechanical calculations, we have illustrated the energy and the temperature dependence by assuming the crystal to be initially in a low-lying state and calculating the renormalization of the particle wave function using the Debye model for the lattice vibrations. The attenuation is shown to be a natural consequence of the inelastic processes, and its magnitude is found to be small compared to previous conjectures.

### I. INTRODUCTION

Ever since Lindhard<sup>1</sup> proposed the theoretical basis for the channeling of particles in perfect crystals based on the ideas of the strings of atoms and the critical angle, a good deal of experimental work has been done,<sup>2-5</sup> mostly on the channeling of heavy ions in perfect crystals. There has been excellent agreement between experimental and theoretical values of the critical angle, the range of the ions in the crystal, and the other parameters. However, for light particles such as electrons and positrons, Lindhard's classical treatment has been

shown<sup>6,7</sup> to give only the gross features of the phenomena, and it has been found in a quantum-mechanical treatment that the phenomena must show a mass dependence, in contradiction to the classical predictions. Actually, similar deviations from classical results had been pointed out by Lervig *et al.*,<sup>8</sup> who showed that for electrons and positrons the penetration into the classically forbidden region will be significant and the quantum effects must be taken into account. A similar quantum-mechanical treatment of the electron and positron channeling has been proposed by Howie.<sup>9</sup>

The experimental situation for light-particle